Original Article

A Novel CAD System for Mitosis detection Using Histopathology Slide Images

Ashkan Tashk, Mohammad Sadegh Helfroush, Habibollah Danyali, Mojgan Akbarzadeh[1]

Department of Electrical and Electronic Engineering, Shiraz University of Technology, [1]Department of Pathology, School of Medicine, Shiraz University of Medical Sciences, Shiraz, Fars, Iran

ABSTRACT

Histopathology slides are one of the most applicable resources for pathology studies. As observation of these kinds of slides even by skillful pathologists is a tedious and time-consuming activity, computerizing this procedure aids the experts to have faster analysis with more case studies per day. In this paper, an automatic mitosis detection system (AMDS) for breast cancer histopathological slide images is proposed. In the proposed AMDS, the general phases of an automatic image based analyzer are considered and in each phase, some special innovations are employed. In the pre-processing step to segment the input digital histopathology images more precisely, 2D anisotropic diffusion filters are applied to them. In the training segmentation phase, the histopathological slide images are segmented based on RGB contents of their pixels using maximum likelihood estimation. Then, the mitosis and non-mitosis candidates are processed and hence that their completed local binary patterns are extracted object-wise. For the classification phase, two subsequently non-linear support vector machine classifiers are trained pixel-wise and object-wise, respectively. For the evaluation of the proposed AMDS, some object and region based measures are employed. Having computed the evaluation criteria, our proposed method performs more efficient according to f-measure metric (70.94% for Aperio XT scanner images and 70.11% for Hamamatsu images) than the methods proposed by other participants at Mitos-ICPR2012 contest in breast cancer histopathological images. The experimental results show the higher performance of the proposed AMDS compared with other competitive systems proposed in Mitos-ICPR2012 contest.

Key words: *Automatic mitosis detection system, completed local binary pattern, histopathology, maximum likelihood estimation, object- and pixel-wise feature extraction, support vector machine*

INTRODUCTION

Early years of the last century with the pervasive attention paid to diseases such as various types of cancers, pathologists and clinicians have moved toward proposing some aiding careers for better diagnosis (disease identification), prognosis (disease evolution outcomes prediction) and theragnosis (therapy outcomes prediction). One of such careers is based on the study of carcinoma tissues and their related characteristics. To discriminate and highlight these features, special techniques such as fixing the biopsied tissue by formalin, tissue processing, sectioning and staining them by a different type of organic dyes such as hematoxyline and eosin (H and E) are employed by pathologists.[1] The breast cancer pathology slides are also the results of H and E stained paraffin-fixed blocks of breast biopsied tissue specimens. In the continuous of such studies, pathologists use microscopic observations usually with diverse resolution frames obtained using microscopic acquisition to grade the carcinoma. In particular for breast cancer grading, there is a popular grading system named as Elston and Ellis or Nottingham grading system (NGS) which is a modified version of previous standard system, Scarff, Bloom and Richarson.[2] NGS is highly recommended by World Health Organization as the most organized and feasible grading system for breast cancer.[3,4] In NGS, three morphological components must be assessed by pathologists: (a) Tubule formation (TF), (b) nuclear pleomorphism score (NPS) (based on nuclei size, shape, chromatin intensity and localization) and (c) mitotic counting. Mitosis count (MC) score represents the number of Mitoses, i.e., the number of dividing nuclei in four phases). MC is assessed in the peripheral areas of the neoplasm. It is based on the number of mitoses per 10 high power fields (HPFs) which usually equals with ×40 magnification frames, i.e., high resolution frames.[3] MC must be done in a more firm and rigorous fashion than TF's and NPS's. In NGS, mitotic counting is scored according to the number of mitotic figures per 10 consecutively microscopic

HPFs ($\times$40) of histological images as: Score 1: 0-9 mitoses; Score 2: 10-19 mitoses; and Score 3: >19 mitoses.[4,5]

Among all of these factors, the MC is the most complicated and vigorous procedure which needs significantly high profession and better experience for their detection. In spite of great advances in histopathological image analysis by professional pathologists, there are many researches and studies for the establishment of computer-aided diagnosis (CAD) utilities to avoid dispersion in inter- and intra-pathological observations.[6-13]

In one of the most recent proposed methods for automatic detection of mitoses in breast cancer histopathology slide images, the contrast between mitotic pixels and non-mitotic ones are mainly provided by considering the approximated distribution of such pixels[14] in each of HPFs of a histopathology slide image. In fact, in,[14] the main idea for the extraction of mitosis cells and discriminating them from the other type of cells is done by a statistical approach. The statistical approach is based on the guessed (empirically but not logically) distribution of pixels belonging to mitosis and non-mitosis cells in an individual breast cancer histopathology slide image. Due to this fact, the authors of this paper suggested gamma distribution for mitosis cells and Gaussian distribution for the non-mitosis ones. Then, the parameters of these guessed distributions are estimated by expectation maximization (EM) estimation in which there is some specific parameter adjustment necessary for correct estimation. After that, as the results of such estimation has made a significant amount of errors (many number of false positives [FPs]), thus, a separate feature extraction approach is employed to classified the extracted potential mitosis candidates from the non-mitosis ones using a context aware post-processing. Of course, the proposed method is only applied on the scanner A histopathology slide images and the efficiency of the results for this database is about 71% which is near the ones proposed, but our method has less complication and computational complexity than their proposed method Since we use maximum likelihood estimation (MLE) for candidate extraction from filtered and denoized slide images which is faster than EM. Furthermore, our method uses most reliable and robust textural features in both pixel- and object-wise manners, which assures less FP extraction and avoids more false negatives (FNs) simultaneously not independently like the proposed gamma-Gaussian mixture model.

Another proposed method for the whole grading of breast cancer histopathology slide images is proposed by Roullier *et al.* in.[15] The main contribution of this paper is related to the whole grading of a breast cancer histopathology slide image in a four level resolution strategy based on Nottingham grading standard. The MC is done in the 4th level. According to the explanation added by the authors to this reference, frame counting stereological evaluation is conducted to quantify the extraction of mitotic cells.

However due to the sparseness and low number of mitosis for Grade 1 and 2, this type of stereological evaluation is not adapted (results will not be statistically significative) and therefore, the authors have performed the evaluation only for Grade 3 that exhibits much more mitosis.

The main purpose of this paper is concentrated on designation of an authentic automatic mitosis detection CAD for assisting pathologists in MC procedure.

The rest of this paper is organized as follows: In the next section, the materials which herein are histopathology slide images are acquired by means of two different kinds of scanners and the related procedures for the proposed automatic mitosis detection system (AMDS) are introduced. Different kinds of evaluation measures are introduced and implemented over the acquired datasets in the results section. Finally, to analyze, compare and conclude the performance of the proposed AMDS, discussions and conclusion section is added.

MATERIALS AND METHODS

To achieve the desired AMDS, some specific tools are required which must have significantly accurate and reliable information such as ground truth maps and high resolution qualities. For this purpose, specific datasets are used whose origination is described in the following subsection. In addition, the flowchart-like scheme of the proposed AMDS is overviewed step by step in the following subsections.

Image Acquisition Materials

The input images to the proposed AMDS are acquired by two different equipments named as Aperio XT scanner with a resolution of 0.2456 μm per pixel and Hamamatsu NanoZoomer scanner with a slightly better resolution of 0.2273 μm (horizontal) and 0.22753 μm (vertical) per pixel so a pixel of scanner H is not exactly a square. The resolutions of these two scanners and their acquired digital image sizes are listed in Table 1. According to these two kinds of scanners, a set of 5 breast cancer biopsy slides have been used which are provided by Prof. Frédérique Capron and Dr. Catherine Genestie, two experienced pathologists of Pitié-Salpêtrière Hospital in Paris, France.[4] In addition, for each breast cancer histopathology slides, 10 HPF which are equivalent to $\times$40 microscopic magnifications, are selected with the advice of pathological experts. Each HPF has a predefined dimension which cited in Table 1. Note that each mitosis occupies an average space of 300 μm² and this area is acquired with different resolutions by each of the named scanners. Acquiring digital histopathological slide images, it is the time of image processing for managements essential for a computerized aided mitosis detection system. In Figure 1, some histopathological slide images as the samples of Scanners A and H acquired images and their related ground-truth maps for the same patient are depicted.

Proposed AMDS Implementation Stages

Similar to any kind of automatic histopathological image analysis system, the proposed method comprises three basic image processing steps as following: (1) Pre-processing and segmentation,[11] (2) feature extraction and selection[12] and finally (3) disease detection, classification and post-processing.[13] The second phase is testing which includes automatic mitosis detection procedures based on the information achieved during the training phase.

Preprocessing Stage

In the first step of preprocessing based on the proposed method, the acquired histopathological slide images are filtered using 2-D anisotropic diffusion. The causes for using such filtering can be as: (a) Low resolution either in spatial or transform domain; (b) high level of noises; (c) low contrast; (d) geometric deformations; and (e) presence of image artifacts. The functionality of such filters is based on some special partial differential equation whose solutions include some special conductive co-efficient functions (CCFs) computed as follows:[16]

$$C^i(x,y) = [c^i(x^-,y), c^i(x^+,y), c^i(x,y^-), c^i(x,y^+)]^T \qquad (1)$$

Table 1: Resolution of the scanners A and H

Scanner name	Resolution (μm/pixel)	Dimension of HPF to cover an area of 512 μm²×512 μm² (0.262 mm²)	Resolution area of a mitosis (about 30 μm²)
Aperio XT (A)	0.2456	2084 pixels× 2048 pixels	500 pixels
Hamamatsu NanoZoomer (H)	0.2273 horizontal and 0.22753 vertical	2252 pixels× 2250 pixels	580 pixels

HPFs – High power fields

Where C^i (x, y) and $C^i(x^{\mp}, y^{\mp})$ stand for the conductive co-efficient vector and the CCFs or components in step i^{th} of filtering step, respectively.

$$I_{RGB}^{i+1}(x,y) = I_{RGB}^{i+1}(x,y) + \lambda C(x,y)^T \nabla I_{RGB}^i(x,y) \qquad (2)$$

Where $I_{RGB}^{i+1}(x,y)$ stands for the RGB image in step i^{th} of filtering step. λ is the contrast parameter belonging to the interval [0,0.25]. In addition, the definition of $\nabla I_{RGB}^i(x,y)$ and its relation with $C^i(x,y)$ is as the following formula:

$$\nabla I_{RGB}^i(x,y) = [\nabla I_{RGB}^i(x^-,y), \nabla I_{RGB}^i(x^+,y), \nabla I_{RGB}^i(x,y^-),$$
$$\nabla I_{RGB}^i(x,y^+)]^T \qquad (3)$$

$$C^i(x,y) = e^{-\left(\frac{\|\nabla I^i(x,y)\|}{\kappa}\right)^2} \qquad (4)$$

$$C^i(x,y) = \left(1 + \left(\frac{\|\nabla I^i(x,y)\|}{\kappa}\right)^2\right)^{-1} \qquad (5)$$

It is worth mentioning that the CCF in (4) predominates larger regions over the smaller ones whilst the CCF in (5) prefers high contrast edges to the ones with low contrast. In addition, each color channel can only be processed by the proceeding anisotropic diffusion filters separately. The results of different iterative anisotropic diffusion filtering are depicted in Figure 2.

The main morphological procedures are closing and opening of the binary image enhanced from the previous filtering phase as a pre-process. The most common and conventional structuring element used for the employed morphological procedures is a disk with radius 2-3 (depending on the morphology action applied to the binary images) and some other morphology tools such as hole filling, pruning and binary region properties extraction are exerted for making
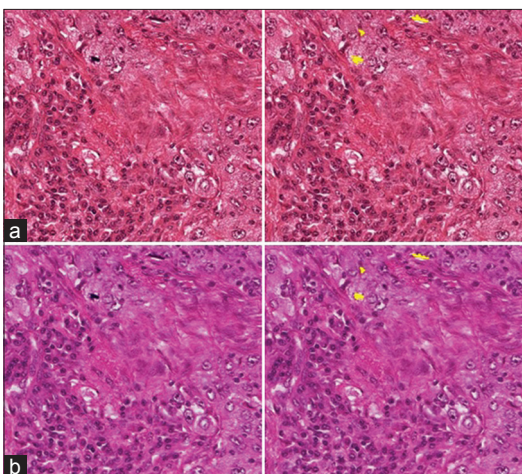

Figure 1: Sample of scanners A and H quarterly histopathological slide images and their related ground-truth maps for the same patient: (a) Original scanner A histopathological slide image and its related ground-truth map, (b) original scanner H histopathological slide image and its related ground-truth map
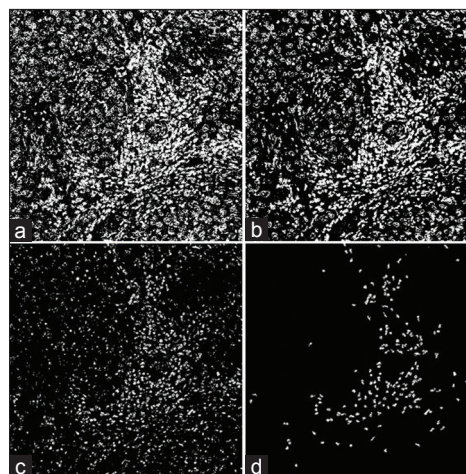

Figure 2: The binary results of a sample histopathology image before and after 2D anisotropic diffusion filtering: (a) Original and simple binarized image, (b-d) binarized images after anisotropic diffusion processing for different numbers of iterative implementations

the segmentation results more reliable and near the reality. In fact, the employed morphological procedures are used before and after segmentation and completed local binary patterns (CLBP) pixel-wise classification phases. After segmentation, the introduced morphology activities lead to the binding of the achieved grains related to glandular mitosis-like objects.

Pixel-wise MLE Stage

In previously proposed methods such as[9] and,[13] the focus is on the features of histology slide images such as object level or spatial related features and their analysis for mitosis detection and consequently MC. In this paper, the proposed method is to extract auxiliary features related to texture of the tissue in histological images.

The role of MLE in the proposed method is to detect potential mitosis candidates including the real mitotic objects and the non-mitotic ones. This target achieves by employing a pixel-wise career for each RGB color planes of digital histopathological images. In this career, a MLE approach is exploited to discriminate foreground from background. For MLE calculations, the posterior probability of each color pixel with its possession to mitosis or non-mitosis area must be computed based on the conditional Bayes' law:

$$P(W_j \mid X) = \prod_{i=R,G,B} \frac{\rho(x_i \mid W_j)\rho(W_j)}{\rho(x_i)} \tag{6}$$

Where $P(W_0 \mid X_{RGB}) = \dfrac{\rho(X \mid W_0)\rho(W_0)}{\rho(X)}$ and $P(W_1 \mid X_{RGB}) = \dfrac{\rho(X \mid W_1)\rho(W_1)}{\rho(X)}$ are the mitosis and non-mitosis posterior

probabilities according to the RGB content of region candidates in the form of binary objects. As maximizing (1) is a time-consuming procedure; therefore, it is preferred to maximizing the following formula:

$$P(W_j \mid X_{RGB}) = \prod_{i=R,G,B} \rho(x_i \mid W_j) \tag{7}$$

Indeed, the MLE helps the pixel-wised extraction of the candidates for mitosis and non-mitosis objects. Figure 3 depicts the sample original and ML estimated graphs for $P(W_0 \mid X_{RGB})$ and $P(W_1 \mid X_{RGB})$.

In the employed MLE, the distributions of the mitotic and non-mitotic pixels are both considered as normal or Gaussian with parameters μ_{W_i} and $\sigma^2_{W_i}$ with the following parametric definitions:

$$p(x \mid \overline{\theta}_{W_0}) \cong N(\mu_{W_0}, \sigma^2_{W_0})\, \overline{\theta}_{W_0} = \left[\mu_{W_0}, \sigma^2_{W_0}\right] \tag{8}$$

$$p(y \mid \overline{\theta}_{W_1}) \cong N(\mu_{W_1}, \sigma^2_{W_1})\, \overline{\theta}_{W_1} = \left[\mu_{W_1}, \sigma^2_{W_1}\right] \tag{9}$$

The ML estimation of the mitosis and non-mitosis distributions' parameter vectors $\overline{\theta}_{W_1}$ and $\overline{\theta}_{W_0}$ are calculated as the following formulas:

$$\frac{\partial p(x \mid \overline{\theta}_{W_0})}{\partial \overline{\theta}_{W_0}} = \begin{bmatrix} \dfrac{\partial p(y \mid \overline{\theta}_{W_0})}{\partial \mu_{W_0}} \\ \dfrac{\partial p(y \mid \overline{\theta}_{W_0})}{\partial \sigma^2_{W_0}} \end{bmatrix}, \frac{\partial p(x \mid \overline{\theta}_{W_1})}{\partial \overline{\theta}_{W_1}} = \begin{bmatrix} \dfrac{\partial p(y \mid \overline{\theta}_{W_1})}{\partial \mu_{W_1}} \\ \dfrac{\partial p(y \mid \overline{\theta}_{W_1})}{\partial \sigma^2_{W_1}} \end{bmatrix} \tag{10}$$

The above formulas are computed due to the related optimization principal which states that the global extremes of an objective function match the zeros of its differentiation. According to this description, the following formulas can be computed for the estimated unknown parameters μ_{W_i} and $\sigma^2_{W_i}$ of each pixels class:

$$\mu_{W_i} = \frac{1}{N_{W_i}} \sum_{k_i=1}^{N_{W_i}} P_{k_i} \tag{11}$$

$$\sigma^2_{W_i} = \frac{1}{N_{W_i}} \sum_{k_i=1}^{N_{W_i}} \left(P_{k_i} - \mu_{w_i}\right)^2 \tag{12}$$
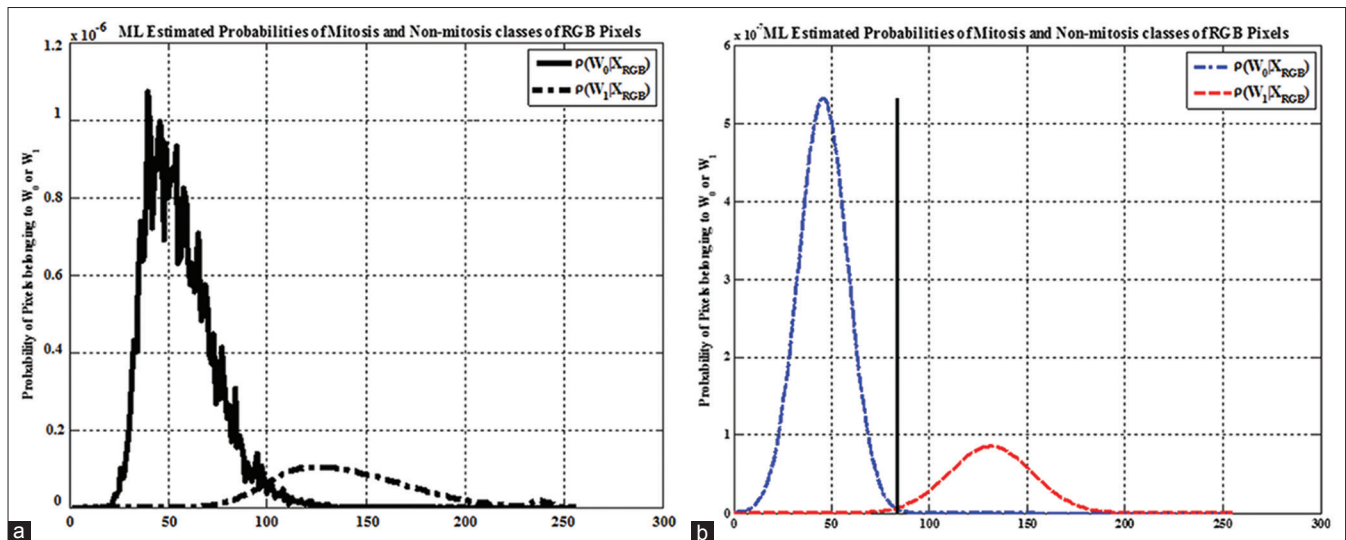

Figure 3: Histogram of the employed maximum likelihood estimation (a) before and (b) after estimation

where P_{k_i} stands for the pixels belonging to the class W_i, $i = 0, 1$.

It is very important that these segmentation procedures leads to the extraction of all possible objective candidates as mitosis ones in foreground, therefore there are not only mitoses among the segmented areas but also there are some other objects such as lymphocytes, blood spots and some other confusingly objects segmented along with mitoses which must be removed during the classification procedure. Furthermore, in some previously proposed methods such as the one proposed in[17] by Viola *et al.*, a "cascade" manner of features are employed which is more complicated than other kinds of feature arrangements. For achieving to the purpose of providing suitable classification, specific and reliable features must be extracted from all objects and then a robust and near optimum classifier has to be employed for discriminating mitotic cells from non-mitotic ones. The next subsections are related to these facts.

Object-wise CLBP Texture Features

The most important textural features extracted from predefined and training mitoses are the most significant CLBP components, i.e., the sign and magnitude of CLBP.[18]

The benefits and priorities of these features return to their simple computation and also their specific statistical modalities. The CLBP can be computed for different neighboring radius (R) and number of pixels (P). Moreover, Figure 4 presents the arithmetic mechanism for computing sign and magnitude elements for CLBP feature vectors. In fact, the LBP sign and magnitude of a given pixel in a digital histological image in a neighborhood with determined R and P can be computed as the following:[18]

$$LBP\_S_{R,P} = \sum_{l=0}^{P-1} s(g_l - g_c)2^l , s(x) = \begin{cases} 1, & x \geq 0 \\ 0, & x < 0 \end{cases} \quad (13)$$

$$LBP\_M_{R,P} = \sum_{l=0}^{P-1} t(g_l, g_c)2^l , t(x,c) = \begin{cases} 1, & x \geq c \\ 0, & x < c \end{cases} \quad (14)$$

The previously proposed CLBP algorithm is only applied to blocks of images. In this paper, we developed a new CLBP platform which is able to compute the sign and magnitude components of an object in a candidate region of a histology slide image. The priority of object-wise CLBP extraction is in two aspects: First, the processed objects never has overlap over the other ones but bounding boxes in the form of blocks may cause aliasing distortion of mitosis and non-mitosis objective candidates acquired from the MLE phase. Second, the extracted CLBP features can be fussed with some other
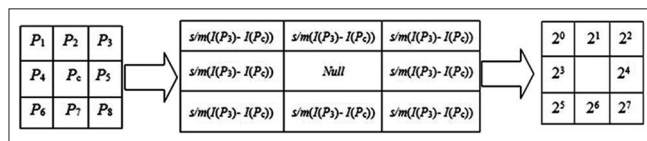
textural feature analysis such as entropy moments with no doubt about their consistency. The arrangement and combination of the features can be various. For instance, the extracted feature vectors from each CLBP components, i.e., sign and magnitude features can be combined with each other in either joint or concatenate manners for the whole RGB color channels. These arrangements affect both computational complexity and classification convergence time-consuming. In fact, the advantages of CLBP is deduced by statistical considerations for both sign and magnitude components. The sign component s_p follows a Bernoulli distribution $Q(n) = b^{\frac{n+1}{2}}(1-b)^{\frac{1-n}{2}}$ with $b = 0.5$ and $n \in \{-1, 1\}$ whilst the magnitude or difference component m_p obeys a single-side Laplace distribution $Q(n) = e^{(-n/\lambda)}/\lambda$, $n \geq 0$. After some mathematical calculation, it is derived that $E_s = \lambda^2$ and $E_m = 4\lambda^2$. These results show that s_p and m_p can preserve more textural features which lead to better pattern recognition performance.

Support Vector Machine: Supervised Classifier

At last, a suitable classifier must be used which has not the high computational complexity like back propagation Neural networks and also not be combined from week classifier like Adaboost.[19] According to such considerations, SVM is chosen as the convenient and also a conventional classifier. The responsibility of SVM classifier is to differentiate between the feature vectors derived from developed pixel-wise MLE stage and object-wise CLBP. In general, SVM is a classifier which is the outcome of solving the following optimization problem:[20]

$$\min_{w,b,\xi} \frac{1}{2}W^TW + C\sum_{i=1}^{m}\xi_i \quad (15)$$

where $\xi_i \geq 0$, $i = 1, \ldots, m$.[20] Figure 5 depicts the concatenation of object-wise extracted CLPB feature vectors for each color channel to be considered as the input elements of the SVM classifier.

Mitosis and non-mitosis object vectors are given to SVM to be trained and in the test stage, the candidates regions are classified as a container of either mitosis or non-mitosis objects. Moreover, the employed SVM is a non-linear
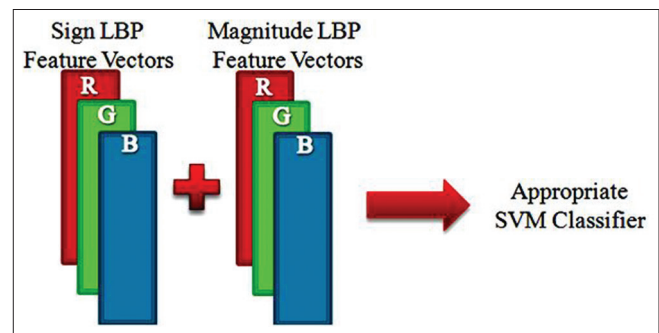

Figure 5: Combination and arrangement of completed local binary patterns feature

Figure 4: Schematic of typical local binary patterns sign and magnitude computations for R = 1 and P = 8

classifier with a polynomial kernel from order $P > 4$ and less than 20 for object-wise feature vectors classification and a radial basis function kernel with parameter $k = 0.1$ exerted for pixel-wise classification purposes.

Proposed Method Review

As a brief review, the proposed automatic mitosis detection method includes the following stages in training and test phases: (1) Pre-processing such as morphological and 2D anisotropic diffusion processes, (2) MLE, (3) textural feature extraction using CLBP and (4) SVM classification based on the local and textural features extracted from histopathology slide images. The sequence of these stages depends on different factors such as the following: In which phase it is located and also for which purpose it is exploited. In general, a schematic block diagram of the two-phase AMDS is shown in Figure 6 in which the implementation stages and their inter- and intra-interactions are illustrated.

RESULTS

After applying the trained system to the test datasets, the results shown in the Tables 2-7 and are achieved. Moreover, Figure 7 illustrates the visual results of implementing the proposed method on two histopathological slide images for both set A and set H.

Definition of Evaluation Metrics

These metrics can be divided into different categories. The most important and useful evaluation metrics are either object or region based measures.

Object-based Evaluation Metrics

To analyze these results and in fact to analyze the performance of the proposed AMDS especially in the phase of classification, it is essential to employ some useful quantitative statistical metrics such as true positive rate (TPR), positive predictive value (PPV) and the effectiveness F-measure as object based metrics defined as in the following formulas:[21]

True positive = Number of true objects detected

FP = Number of objects detected incorrectly

FN = Number of objects rejected or undetected incorrectly

True negative (TN) = Number of objects rejected falsely.

$$\text{Recall or sensitivity} \left(\text{TPR} \right) = \frac{TP}{(TP + FN)} \qquad (16)$$
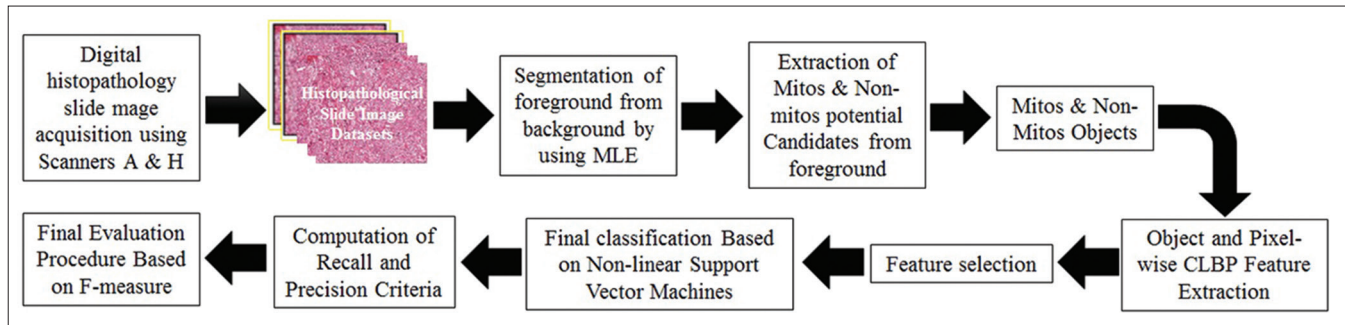

Figure 6: Training and test phases of proposed automatic mitosis detection method

Table 2: Implementation results of the proposed method for the test set A of histology slide images

Parameters	Dataset														
	A00_00	A00_08	A01_04	A01_06	A01_09	A02_00	A02_01	A02_03	A02_07	A03_00	A03_01	A03_04	A04_03	A04_07	A04_09
(TP+FN)	6	2	11	4	9	3	2	1	4	19	9	12	9	5	4
TP	2	2	9	4	7	3	2	0	2	13	7	7	7	4	3
FP	10	2	5	3	1	2	0	0	1	2	0	2	1	1	1
FN	4	0	2	0	2	0	0	1	2	6	2	5	2	1	1

TP – True positive; FP – False positive; FN – False negative; TN – True negative

Table 3: Implementation results of the proposed method for the test set H of histology slide images

Parameters	Dataset														
	H00_00	H00_08	H01_04	H01_06	H01_09	H02_00	H02_01	H02_03	H02_07	H03_00	H03_01	H03_04	H04_03	H04_07	H04_09
TP+FN	6	2	11	4	9	3	2	1	4	19	9	12	9	5	4
TP	6	2	1	1	6	3	2	0	2	14	6	7	5	4	2
FP	0	1	0	0	1	2	0	1	2	1	0	2	2	1	0
FN	0	0	10	3	3	0	0	1	2	5	3	5	4	1	2

TP – True positive; FP – False positive; FN – False negative; TN – True negative
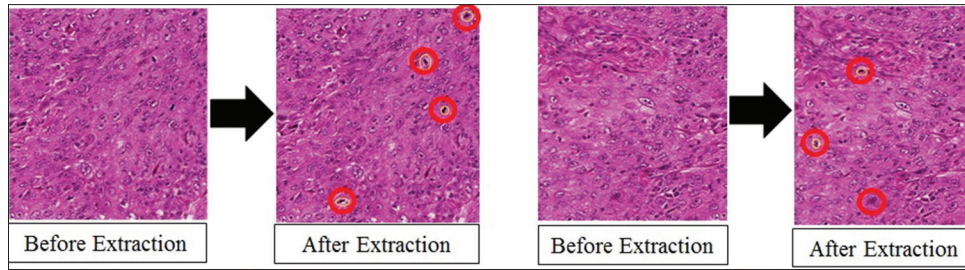
Figure 7: Sample of histopathology slide images before and after proposed automatic mitosis detection employment for (a) scanner A and (b) scanner H

Table 4: Evaluation results of the proposed method for the test set A of histology slide images due to region-based metrics

Test frames	Local mean	Local standard deviation	Nb Pts. inter	Nb Pts. seg	Nb Pts. gt	Area overlap	Area recall	Area specificity	Area precision	Area F-measure
A00_00	0.822	0.738	953	33	286	0.749	0.769	0.9999	0.9665	0.8566
A00_08	1.743	0.233	650	759	40	0.449	0.942	0.9998	0.4613	0.6193
A01_04	2.460	5.766	5116	2291	1991	0.544	0.720	0.9994	0.6906	0.7050
A01_06	2.688	3.152	2818	1294	1098	0.541	0.720	0.9997	0.6853	0.7020
A01_09	1.156	1.297	4716	2825	788	0.566	0.857	0.9993	0.6254	0.7230
A02_00	0.943	0.312	1372	1935	0	0.415	1	0.9995	0.4149	0.5864
A02_01	1.128	0.449	1261	870	62	0.575	0.953	0.9998	0.5917	0.7302
A02_03	0	0	0	0	0	0	0	1	0	0
A02_07	0.939	0.206	728	1039	0	0.412	1	0.9997	0.4120	0.5836
A03_00	2.269	4.084	5098	4971	701	0.473	0.879	0.9988	0.5063	0.6426
A03_01	1.338	2.339	2531	3212	128	0.431	0.952	0.9992	0.4407	0.6025
A03_04	1.106	1.242	2863	3103	73	0.474	0.975	0.9992	0.4799	0.6432
A04_03	1.675	3.654	4055	2679	864	0.534	0.824	0.9993	0.6022	0.6960
A04_07	0.861	0.650	2689	1786	78	0.591	0.972	0.9995	0.6009	0.7426
A04_09	1.672	2.174	2760	1815	288	0.568	0.906	0.9995	0.6033	0.7241

Table 5: Complete list of participating research groups in the Mitos-ICPR2012 contest for Aperio XT Images according to the recall, precision and F-measure (F-score)

Participant group name	Precision	Recall	F₁-score
IDSIA[23]	0.88	0.70	0.782
IPAL[24]	0.69	0.74	0.718
SUTECH	0.70	0.72	0.709
NEC[25]	0.74	0.59	0.659
UTRECHT[26]	0.51	0.68	0.583
WARWICK[14]	0.46	0.57	0.513
NUS	0.63	0.40	0.490
ISIK[28]	0.28	0.68	0.397
ETH[27]	0.14	0.80	0.374
OKAN	0.78	0.22	0.343
IITG	0.17	0.46	0.255
DREXEL	0.14	0.21	0.172
BII	0.10	0.32	0.156
QATAR	0.0	0.94	0.005

$$\text{Precision } (PPV) = \frac{TP}{(TP+FN)} \qquad (17)$$

Harmonic mean of precision and recall is a reliable and conventional metric for assessment of object- and region-based criteria.

$$\text{F-measure}_\gamma = (1+\gamma^2)\frac{Precision \times Recall}{\gamma^2 \times Recall + Precision} \qquad (18)$$

or

Effectiveness F-measure (relative weight $0 < \beta < 1$): This metric allows weighting the relevance of a correct classification:[21]

$$\text{Effective F-measure}_\beta = \frac{TPR \times PPV}{(1-\beta)\times TPR + \beta \times PPV} \qquad (19)$$

In contrast, the performance of the annotation tasks, i.e., the identification of the concepts presented in an image with multiple biological concepts, was quantified in terms of its sensitivity, or TPR, specificity or TN rate and accuracy as:

$$\text{Specificity } (SPC) = \frac{TN}{(FP+TN)} \qquad (20)$$

$$\text{Accuracy } (ACC) = \frac{(TP+TN)}{(TP+FP+TN+FN)} \qquad (21)$$

Region-based evaluation metrics

As the proposed method declares, the CLBP feature extraction is applied object-wise to the potential mitosis candidates derived from the proposed segmentation procedure. Therefore, the assessment of the truly extracted and distinguished objects with the ones in the ground truth

Table 6: Evaluation results of the proposed method for the test set H of histology slide images due to region-based metrics

Test frames	Local mean	Local standard deviation	Nb Pts. inter	Nb Pts. seg	Nb Pts. gt	Area overlap	Area recall	Area specificity	Area precision	Area F-measure
H00_00	1.644	1.678	3457	1678	783	0.584	0.815	0.9997	0.673	0.737
H00_08	1.224	1.326	647	410	211	0.510	0.754	0.9999	0.612	0.676
H01_04	4.911	0	258	55	403	0.360	0.390	0.9999	0.824	0.530
H01_06	1.482	0	1744	289	205	0.779	0.895	0.9999	0.858	0.876
H01_09	2.226	3.427	3419	1378	1855	0.514	0.648	0.9997	0.713	0.679
H02_00	2.232	2.257	1497	1312	213	0.495	0.875	0.9997	0.533	0.663
H02_01	1.598	0.326	1399	570	193	0.647	0.879	0.9999	0.711	0.786
H02_03	0	0	0	0	0	0	0	1	0	0
H02_07	1.068	0.135	947	765	0	0.553	1	0.9998	0.553	0.712
H03_00	1.793	3.483	6115	5008	629	0.520	0.907	0.9990	0.550	0.685
H03_01	1.337	1.007	2512	2375	73	0.506	0.972	0.9995	0.514	0.672
H03_04	1.102	1.282	2848	2703	40	0.509	0.986	0.9995	0.513	0.675
H04_03	2.810	3.210	3735	696	2397	0.547	0.609	0.9999	0.843	0.707
H04_07	1.076	0.507	2968	392	1502	0.610	0.664	0.9999	0.883	0.758
H04_09	2.264	0.5608	2796	766	609	0.670	0.821	0.9998	0.785	0.803

Table 7: Complete ranking list of participating research groups in the Mitos-ICPR2012 contest for Hamamatsu images according to the recall, precision and F-measure (F-score)

Participant group name	Precision	Recall	F_1-score
SUTECH	0.8243	0.61	0.7011
IPAL[24]	0.5591	0.71	0.6256
NEC[25]	0.7586	0.44	0.5570
DEFINIENS	0.4615	0.30	0.3636

map is done based on a state of the art region growing based method. Two segmentation similarity indices (the Zijdenbos and the Jaccard) exist to measure the segmentation performance. The Zijdenbos similarity index (ZSI) as shown by Zijdenbos *et al.*,[22] is a well-known metric for performance assessment of any region-based segmentation method. It measures the percentage of the overlapping ratio between the two shapes automatic segmented area and manually segmented area. ZSI is defined as:

$$\text{ZSI} = 2 \times \frac{|A(S) \cap A(G)|}{|A(S)| + |A(G)|} \tag{22}$$

where A (S) and A (G) are the generated binary image by the proposed method and the ground truth objects selected manually by the pathologists, respectively.

In addition to ZSI, the Jaccard similarity index (JSI) and other related indices are also calculated to provide comprehensive evaluation of the method. The JSIs which deal with the surface of the objects, are defined as the following formulas:

$$\text{Overlap}(\text{JSI}) = \frac{|A(S) \cap A(G)|}{|A(S) \cup A(G)|} \tag{23}$$

$$\text{Sensitivity} = \frac{|A(S) \cap A(G)|}{|A(G)|} \tag{24}$$

$$\text{Specificity} = \frac{|N - A(S) \cup A(G)|}{|N - A(G)|} \tag{25}$$

$$\text{PPV} = \frac{|A(S) \cap A(G)|}{|A(S)|} \tag{26}$$

where N, A (S) and A (G) are the total number of pixels in HPF, the area of extracted mitosis and the area of ground truth mitosis, respectively. $|A(S)|$ and $|A(G)|$ are the number of pixels of the area of segmented and ground truth mitoses, respectively.

There are some other region-based (segmentation) error indices which are calculated as follows:

$$\text{Extra Fraction} = \frac{(N - A(G)) \cap A(S)}{A(G)} \tag{27}$$

$$\text{Miss Fraction} = \frac{A(G) \cap (N - A(S))}{A(G)} \tag{28}$$

where $A(S)$ and $A(G)$ have the same definition as employed in the previous formulas.

Evaluation Metrics Implementation

These subjective evaluation metrics are used to assess the accuracy and efficiency of the proposed AMDS. Pathologists also assess their researches in the field of histopathology studies according to their objective assessment criteria, but their analysis is issued based on the subjective metrics. According to these measurements, the results shown in Tables 4 and 5 are achieved which include both region- and object-based measures for the A and H and evaluation datasets.

DISCUSSION AND CONCLUSION

These subjective evaluation metrics are used to assess the accuracy and efficiency of the proposed AMDS. Pathologists

also assess their researches in the field of histopathology studies according to their objective assessment criteria, but their analysis is issued based on the subjective metrics. According to these metrics, the results shown in Tables 4 and 5 are achieved. The results shown in Tables 6 and 7 are achieved due to the region-based measures for the A and H and evaluation datasets.

Discussions

In this subsection, two distinct aspects are considered for analysis. First, the most successful proposed methods participated at Mitos-ICPR2012 contest are analyzed and discussed. Then, the evaluation results achieved by the proposed AMDS in this paper have been concluded.

Comparison Between the Proposed Method and Competitive Ones

As mentioned before, the proposed AMDS has competed with some other proposed method based on an international contest introduced as Mitos-ICPR2012. According to the contest results and also the abstract of the other proposed methods, it can be inferred that the proposed method of this paper has the following differences with those ones in the ranks near it:

- Image and Pervasive Access Lab (IPAL)[24] proposed a method for AMDS based on only a single color channel in order to reduce complexity and also data length reduction. They have also employed the following procedures for their presented AMDS: Detection of candidate regions based on blue ratio, Laplacian of Gaussian, thresholding and morphological operations and extraction of first and second order statistics features for segmenting regions of selected candidate and at the last phase, classification of the extracted feature vectors. According to their deduction, the classification performance was poor while employing all extracted features for classification of mitosis and non-mitosis region. That is because of irrelevancy and redundancy of those whole features
- NEC[25] research group proposed a method for AMDS in which the features of nuclei such as color, texture and shape information of segmented regions around the nuclei are extracted by a conventional neural network (CNN), processed them by Principal Components Analysis (PCA) due to RGB color channels and finally classified feature vectors by a SVM with a variety of kernels from linear to cubic polynomial models. This method suffers from two deficiencies: First, a CNN is used for extraction of features which is complicated and may have highly computational complexity and secondly the classifier is done over the reduced size feature vectors because of applying of PCA to the extracted RGB features
- DEFINIENS presents a Cognition Network Technology application combined with standard data mining

methods to describe shape and color of mitotic phases and other related properties. For the complex problem of mitosis detection, they combine their proposed method with the standard classification and regression tree algorithm. The implementation results demonstrate that in spite of their proposed method complexity, it is not as efficient as it is expected
- IDSIA[23] research group claims that they solve the problem of Mitosis detection in Histological Images (MITOS dataset) by means of pixel classifiers. However, their proposed method is highly depends on the content of and integrity of the digital histopathology slide images and therefore can only performs successful for the images acquired by A scanner.

All other proposed methods by the rest participating groups also suffer from some specific shortcoming which leads to the results depicted in Charts 1 and 2.

Evaluation Results Discussion

As the results of the Mitos-ICPR2012 contest shows, the proposed AMDS has better performance than the other competitive methods, especially due to the f-measure metrics. In addition, the region-based metrics demonstrate the spatial accuracy of this method for seeking and tracking found mitoses. In general, the proposed method is in an acceptable level of accuracy, robustness and reliability.

The results shown in Tables 2-7 are reported and evaluated by the Mitos-ICPR2012 contest holder. In general, Tables 2 and 3 indicate the ability of the proposed method for detecting mitosis objects and also its ability to discriminate mitosis from non-mitosis objects correctly for both dataset images acquired by scanner A and H, respectively. On the other hand, Tables 4 and 6 comprise the region-based detection capability of the proposed method for both scanners A and H. The competitive results of the proposed method in comparison with other contestants at Mitos-ICPR2012 for scanners A and H are listed in Tables 5 and 7, respectively. As it can be seen, the proposed method is between the first three winners of the Mitos-ICPR2012 contests, third for scanner A and first for scanner H. Again, it is worth to remind that the results are evaluated and reported by the sponsors and holders of the accredited Mitos-ICPR2012.

CONCLUSION

The evaluation and implementation results demonstrate that the proposed automatic mitosis detection algorithm based on textural features extracted from histopathological slide images is an efficient and feasible method for mitosis detection and consequently counting. In the proposed method, some important notes are considered such as usage of sign and magnitude CLPB feature vectors in concatenate manner instead of joint mode.
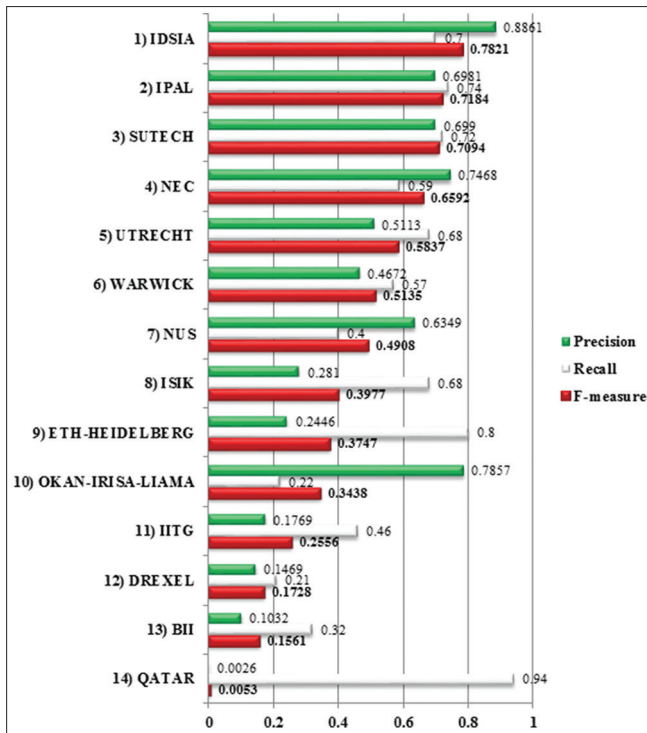
Chart 1: Complete list of participating research groups in the Mitos-ICPR2012 contest for Aperio XT images according to the recall, precision and F-measure (F-score)

About the novelty of the proposed method in this paper, it can be declared that the old CLBP is only based on region-wise local binary features extraction, whereas in our proposed method, the CLBP features are extracted object-wise, exactly matched with the main purpose of mitosis objects discrimination from those ones which must not be mistaken with mitoses such as apoptotic cells – programed death cells – and hyper chromatins – abnormally but not sickeningly inflamed cells. The empirical experiments such as the Mitos-ICPR2012 contest lead to results which verify the noticeable signification and efficiency of the proposed CLBP feature extraction approach toward automatic mitosis detection goal from digital histopathology slide images.

All of the proposed method considerations lead to the results indicated in the implementation tables. It is worth mentioning that our proposed method has achieved successful results in the international contest held by IPAL in association with IEEE ICPR2012 conference. The proposed method had reached to the f-measure of more than 70% for the Aperio XT scanner dataset which placed at the third rank. Moreover, the proposed automatic detection method succeeded to achieve the first place for the results related to its implementation over Hamamatsu Zoomer Scanner dataset. The gained f-measure for this scanner was exactly 70.11% which was the first among the other contestant ones.
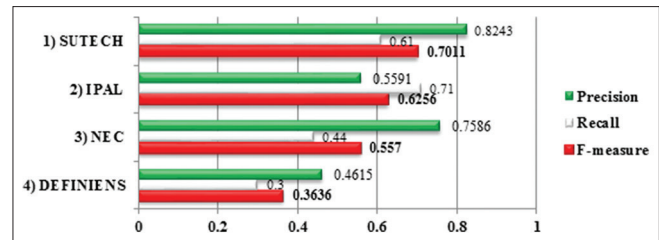

Chart 2: Complete ranking list of participating research groups in the Mitos-ICPR2012 contest for Hamamatsu images according to the recall, precision and F-measure (F-score)

ACKNOWLEDGMENTS

REFERENCES

1. He L, Long LR, Antani S, Thoma GR. Histology image analysis for carcinoma detection and grading. Comput Methods Programs Biomed 2012;107:538-56.

2. Elston CW, Ellis IO. Pathological prognostic factors in breast cancer. I. The value of histological grade in breast cancer: Experience from a large study with long-term follow-up. Histopathology 1991;19:403-10.

3. Tutac AE, Racoceanu D, Leow WK, Dalle JR, Putti T, Xiong W, *et al*. Translational approach for semi-automatic breast cancer grading using a knowledge-guided semantic indexing of histopathology images. Proc. MIAAB 2008; p. 1-8.

4. Dataset for mitosis detection in breast cancer histological images: An ICPR 2012 contest. Available from: http://www.ipal.cnrs.fr/ICPR2012/. [Last accessed on 2014 Jan 16].

5. Tutac A. Histological grading on breast cancer. IPAL Internal Report 2007, MIIRAD/IPAL – Breast cancer grading (BCG), 2007.

6. ten Kate TK, Beliën JA, Smeulders AW, Baak JP. Method for counting mitoses by image processing in Feulgen stained breast cancer sections. Cytometry 1993;14:241-50.

7. Petushi S, Garcia FU, Haber MM, Katsinis C, Tozeren A. Large-scale computations on histology images reveal grade-differentiating parameters for breast cancer. BMC Med Imaging 2006;6:14.

8. Kong J, Sertel O, Shimada H, Boyer K, Saltz J, Gurcan M. Computer-aided grading of neuroblastic differentiation: Multi-resolution and multi-classifier approach. IEEE Proceeding of International Conference on Image Processing (ICIP), 2007.

9. Doyle S, Agner S, Madabhushi A, Feldman M, Tomaszewski J. Automated grading of breast cancer histopathology using spectral clustering with textural and architectural image features. IEEE Proceeding on International Symposium on Biomedical Imagery (ISBI), 2008.

10. Roullier V, Ta VT, Lézoray O, Elmoataz A. Graph-based multi-resolution segmentation of histological whole slide image. IEEE Proceeding on International Symposium on Biomedical Imagery (ISBI), 2010.

11. Roullier V, Lézoray O, Ta VT, Elmoataz A. Multi-resolution graph-based analysis of histopathological whole slide images: Application to mitotic cell extraction and visualization. Comput Med Imaging Graph 2011;35:603-15.

12. Huh S, Ker DF, Bise R, Chen M, Kanade T. Automated mitosis detection of stem cell populations in phase-contrast microscopy images. IEEE Trans Med Imaging 2011;30:586-96.

13. Hsu CW, Chang CC, Lin CJ. A practical guide to support vector classification, 2010. Available from: http://www.csie.ntu.edu.tw/~cjlin; 2010.

14. Khan AM, Eldaly H, Rajpoot NM. A gamma-gaussian mixture model for detection of mitotic cells in breast cancer histopathology images. J

Pathol Inform 2013;4:11.

15. Roullier V, Lézoraya O, Vinh-Thong T, Elmoataz A. Multi-resolution graph-based analysis of histopathological whole slide images: Application to mitotic cell extraction and visualization. Comput Med Imaging Graph 2011;35;603-15.

16. Perona P, Malik J. Scale-space and edge detection using anisotropic diffusion. IEEE Trans Pattern Anal Mach Intell 1990;12:629-39.

17. Viola P, Jones M. Rapid object detection using a boosted cascade of simple features. IEEE Conf Comput Vis Pattern Recognit 2001;1:511-8.

18. Belsare AD, Mushrif MM. Histopathological image analysis using image processing techniques: An overview. Signal Image Process Int J 2012;3:23-36.

19. Guo Z, Zhang L, Zhang D. A completed modeling of local binary pattern operator for texture classification. IEEE Trans Image Process 2010;19:1657-63.

20. Daskalaki S, Kopanas I, Avouris N. Evaluation of classifiers for an uneven class distribution problem. Appl Artif Intell 2006;20:381-417.

21. Udupa JK, Leblanc VR, Zhuge Y, Imielinska C, Schmidt H, Currie LM, *et al*. A framework for evaluating image segmentation algorithms. Comput Med Imaging Graph 2006;30:75-87.

22. Zijdenbos AP, Dawant BM, Margolin RA, Palmer AC. Morphometric analysis of white matter lesions in MR images: Method and validation. IEEE Trans Med Imaging 1994;13:716-24.

23. Ciresen DC, Giusti A, Gambardella LM, Schmidhuber J. Mitosis detection in breast cancer histology images with deep neural networks. 15th International Conference on Medical Image Computing and Computer Assisted Intervention (MICCAI2012), Nice, France, 1-5 October, 2012.

24. Irshad H, Jalali S, Roux L, Racoceanu D, Hwee LJ, Naour GL, *et al*. Automated mitosis detection using texture, SIFT features and HMAX biologically inspired approach. J Pathol Inform 2013;4:S12.

25. Malon CD, Cosatto E. Classification of mitotic figures with convolutional neural networks and seeded blob features. J Pathol Inform 2013;4:9.

26. Veta M, van Diestb P, Pluim J. Detecting mitotic figures in breast cancer histopathology images. In: Proceedings of SPIE Medical Imaging. Proc. SPIE 8676, Medical Imaging 2013: Digital Pathology, 867607 (March 29, 2013); doi:10.1117/12.2006626.

27. Tek FB. Mitosis detection using generic features and an ensemble of cascade adaboosts. J Pathol Inform 2013;4:12.

28. Sommer C, Fiaschi L, Heidelberg H, Hamprecht F, Gerlich D. Learning-based mitotic cell detection in histopathological images. Proc. of 21st International Conference on Pattern Recognition (ICPR2012), Tsukuba, Japan, 2012.

BIOGRAPHIES

Ashkan Tashk received his B.Sc. and M.Sc. degrees in Electrical Engineering respectively from Shiraz University, Shiraz, Iran, in 2006 and Shiraz University of Technology, Shiraz, Iran, in 2010. He is now a PhD student at the Department of electrical and electronics engineering, in Shiraz University of technology. He has over 25 publications in various fields of signal and image processing. Indeed, He is with 6 years of research experience in the field of digital image processing. He has a special interest in biomedical imagery and developing new CAD systems for breast cancer grading. Currently he focuses on a fully-software mitosis detection system as the main part of his PhD Thesis.

E-mail: a.tashk@sutech.ac.ir

Mohammad Sadegh Helfroush received the B.S. and M.S. degrees in Electrical engineering from Shiraz University, Shiraz, Iran and Sharif University of Technology, Tehran, Iran in 1993 and 1995, respectively. He performed his Ph.D. degree in Electrical Engineering from Tarbiat Modarres University, Tehran, Iran. Currently he is working as associate professor in department of Electrical and Electronics Engineering, Shiraz University of Technology, Shiraz, Iran.

E-mail: ms_helfroush@sutech.ac.ir

Habibollah Danyali received his B.Sc. and M.Sc. degrees in Electrical Engineering respectively from Isfahan University of Technology, Isfahan, Iran, in 1991 and Tarbiat Modarres University, Tehran, Iran, in 1993. From 1994 to 2000 he was with the Department of Electrical Engineering, University of Kurdistan, Sanandaj, Iran, as a lecturer. In 2004 he received his PhD degree in Computer Engineering from University of Wollongong, Australia. He is currently working as an associate professor with the Department of Telecommunication Engineering, Shiraz University of Technology, Shiraz, Iran. His research interests include medical image processing, data hiding, scalable image and video coding and biometrics.

E-mail: danyali@sutech.ac.ir

Mojgan Akbarzadeh-Jahromi received the M.D degree from Shiraz University of Medical Sciences in 1998, specialty in pathology from Tehran University of Medical Sciences in 2009. She has been with the Department of pathology, School of Medicine, Shiraz University of Medical Sciences, since 2009. Her current research activities include GYN and OB pathology, Breast pathology and Dermatopathology.

E-mail: akbarzadeh@sums.ac.ir